

## Magnetic Resonance Imaging System Based on Earth's Magnetic Field

Aleš Mohorič,<sup>1,\*</sup> Gorazd Planinšič,<sup>1</sup> Miha Kos,<sup>1</sup>  
Andrej Duh,<sup>1</sup> and Janez Stepišnik<sup>1,2</sup>

<sup>1</sup>Physics Department, Faculty of Mathematics and Physics,  
University of Ljubljana, Ljubljana, Slovenia  
<sup>2</sup>Institute Josef Stefan, Ljubljana, Slovenia

### ABSTRACT

This article describes both the setup and the use of a system for magnetic resonance imaging (MRI) in the Earth's magnetic field. Phase instability caused by temporal fluctuations of Earth's field can be successfully improved by using a reference signal from a separate Earth's field nuclear magnetic resonance (NMR) spectrometer/magnetometer. In imaging, it is important to correctly determine the phase of the NMR signal. A reference signal of a fixed-frequency oscillator cannot be used since the Larmor frequency changes with time, following temporal fluctuations of Earth's magnetic field. The reference signal frequency and phase, provided by a separate NMR spectrometer, change in the same way as Earth's field, creating thereby, a stable rotating frame of reference for the measured signal. In principle, excellent homogeneity of the magnetic field enables scanning of very large volume samples. Reduction in  $S/N$  ratio due to the weak magnetic field can be partly compensated by the receiving coil design and shielding of electromagnetic pick-up in audio frequency (AF) range. The smallest voxel examined so far is on the order of  $50 \text{ mm}^3$ . Unlike in the case of strong magnetic fields, detection and processing of low frequency signal are less

---

\*Correspondence: Aleš Mohorič, Physics Department, Faculty of Mathematics and Physics, University of Ljubljana, Jadranska 19, 1000 Ljubljana, Slovenia; E-mail: ales.mohoric@wur.nl.

demanding for the electronics. The techniques used and the results of measurements are briefly presented.

*Key Words:* Earth's magnetic field; NMR; Imaging; Spin lock.

## INTRODUCTION

The advent of nuclear magnetic resonance (NMR), originally discovered in 1946 independently by Bloch et al. and Purcell et al.<sup>[1,2]</sup> was followed by the introduction of pulsed NMR.<sup>[3,4]</sup> Magnetic resonance imaging (MRI) was first demonstrated in 1973 by Lauterbur and Mansfield and Granel.<sup>[5,6]</sup> In 1975, Ernst proposed MRI using phase and frequency encoding and the Fourier transform.<sup>[7]</sup> In pulsed NMR, and for the detection of signal (phase detection and averaging), the phase of the signal and pulses is important and must be monitored accurately.<sup>[8-10]</sup> The importance of NMR in a non-uniform magnetic field for the analysis of molecular motion has also been realized<sup>[11-14]</sup> and the technique, such as pulsed gradient spin echo (PGSE) is presently the standard method used to determine dynamical properties of matter, such as diffusion constant.<sup>[15]</sup> Parallel to the development of NMR in a strong magnetic field, the NMR in Earth's magnetic field evolved.<sup>[16-23]</sup>

## EXPERIMENTAL

Typically, NMR experiments are performed in static uniform magnetic fields. Common sources of static magnetic fields are super conducting coils, electromagnets, and permanent magnets. The induced magnetization, and thus the signal, is proportional to the magnitude of the magnetic field. This fact stimulates the use of strong static magnetic fields. The system for MRI described here utilizes Earth's magnetic field. The magnitude  $B_0$  of Earth's magnetic field at the site of the system is about  $50 \mu\text{T}$ . The very uniform field (inhomogeneity on the order of  $10^{-12} \text{T/m}$ ) is aligned  $11^\circ$  west from the north-south geographical axis and inclined  $30^\circ$  from the vertical toward the north, as shown in Fig. 1. The corresponding proton Larmor frequency ( $\omega = \gamma B_0$ ;  $\gamma$  is gyromagnetic ratio) of 2 kHz is in the audio frequency (AF) range. Because the equilibrium magnetization is too weak for NMR experiment, it is enhanced during the polarization interval; duration of this interval depends on the longitudinal relaxation time of the sample and is usually a few seconds long. Besides polarization, NMR experiments comprises a preparation period (excitation of magnetization with oscillating magnetic field and phase encoding with magnetic field gradients) and detection period. The scheme of the components necessary to perform NMR imaging experiments, is shown in Fig. 2. Uniaxial coils (detection, three gradient, AF, and polarizing) constitute the core of the system (Fig. 3).

The polarizing magnetic field is switched off adiabatically; after the polarization the magnetization is aligned in equilibrium direction along  $B_0$ . Thus, the orientation of the polarizing coil (a solenoid 70 cm long and 40 cm in diameter with 650 windings of 3 mm by 4 mm thick copper wire) is not important. Symmetry axis of the polarizing coil lies horizontally and is perpendicular to Earth's magnetic field. The axis coincides

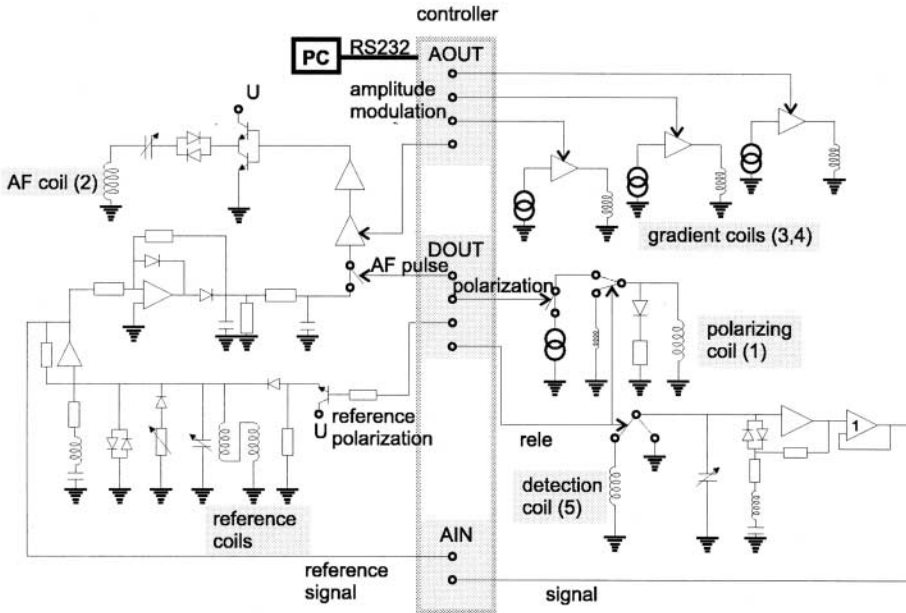


**Figure 1.** The direction of Earth's magnetic field at the site of the NMR imaging system.

with that of the detection coil enabling easy access to the sample area. The polarizing-current source is capable of up to 100 A output at 60 V. In practice, a somewhat lower current of 50 A (optimal duty cycle 2:3) is normally used, producing the magnetic field of 60 mT in the center of the coil. When grounded during the detection period, the polarizing coil acts as a shield against external AF interferences. Optimum shielding is achieved using a suitable inductor connected parallel to the polarizing coil.<sup>[23]</sup> The resistor and the diode connected parallel to the coil prevent the current leakage during the polarization (the applied voltage is negative) and enable the current flow through the resistor during the adiabatic switch off; the coil is critically damped.

The magnetization is excited with AF pulses produced by a solenoid, coiled up in 30 windings, on the inner side of the polarizing coil. It is much larger than the detecting coil so the AF field is uniform across the sample region. The coil is tuned to the Larmor frequency. Two signals are fed into the AF circuit: the first one is the control signal determining the length and the amplitude of the AF pulse. In our case, typical duration of a  $\pi/2$  pulse is a few Larmor periods (about 5 msec). Another input is the free induction signal from the reference coils. The amplitude of this signal decreases exponentially with transverse relaxation of 2 sec. This signal is amplified to get rectangular oscillations, unaffected by transverse relaxation. The harmonic signal is then obtained with a suitable high frequency filter. In a strong field NMR, this signal is provided by a stable frequency oscillator. The envelope of the signal can be controlled enabling soft AF pulses.

After excitation, the magnetization can be manipulated with additional AF pulses and magnetic field gradients produced by gradient coils. The frequency and the phase of the signal are controlled by three orthogonal magnetic field gradients. Three gradient coils produce quadrupole magnetic fields with components parallel to Earth's field, changing

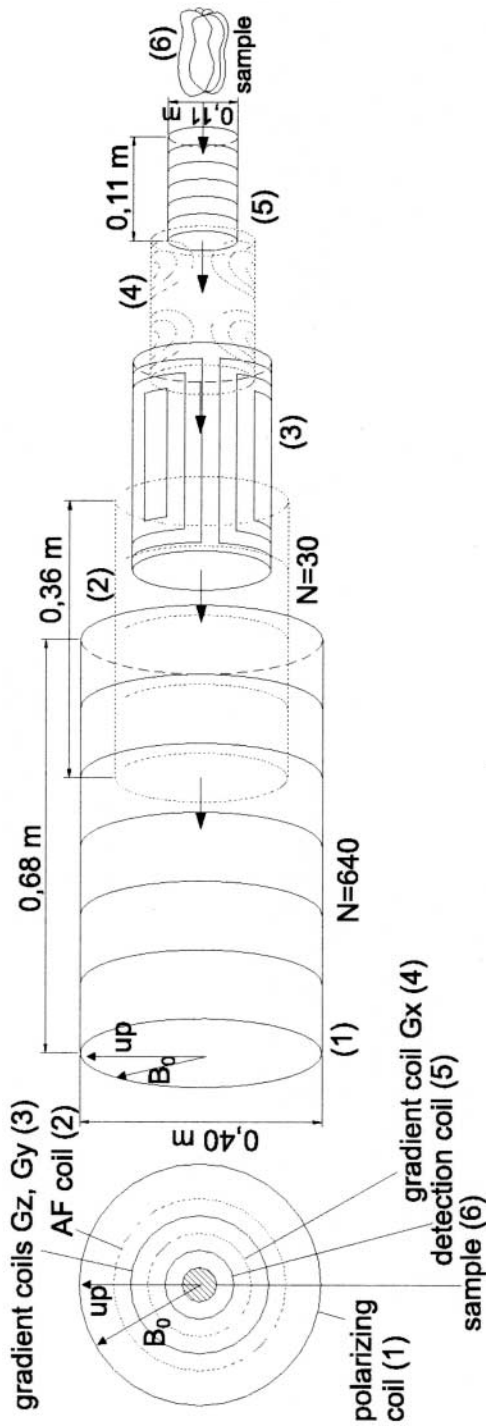


**Figure 2.** Block diagram of the NMR imaging system. The core of the system is the uniaxial coils: detecting, three gradient, AF, and polarizing coil, controlled by a homemade pulse programmer connected to a PC. The reference coil provides the AF signal needed for pulse generation and quadrature detection.

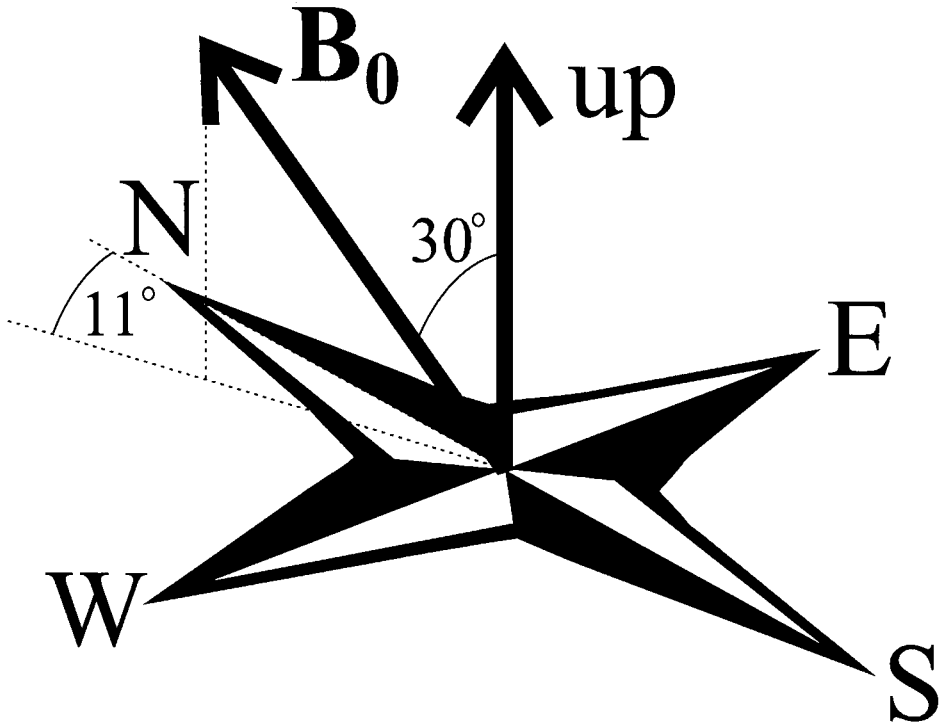


**Figure 3.** The coils of the system; the outermost coil is the polarizing coil and the detecting coil is at the center. The AF and gradient coils are located in between these two. All coils are centered at the same point. The coils are shown in a pullout side view for clarity. The vertical and magnetic field are shown to indicate the orientation of the coils.

linearly in three orthogonal directions:  $z$  gradient (direction along  $B_0$ ),  $x$  gradient (along the symmetry axis of the detection coil), and  $y$  gradient. The gradient coils have low inductance in order to minimize transients.

The gradients in directions perpendicular to the symmetry axis of the detection coil ( $z$  and  $y$  gradient) are produced by quadrupolar coils with straight wires aligned on the surface of a 70 cm long cylinder (diameter 34 cm) with a symmetry axis along  $x$ . The wires are distributed to produce the current density on the surface of the cylinder that varies as  $\sin 2\varphi$  for  $z$  gradient and as  $\cos 2\varphi$  for  $y$  gradient;  $\varphi$  is the polar angle measured from  $z$  axis. The continuous distribution is mimicked by changing the distance between the wires. Each coil is made of four rectangular spirals of 10 windings. The currents in adjacent loops run in the opposite directions. The arcs, completing the loops at the ends of the straight wires, do not contribute significantly to the magnetic field in the probe area. The magnetic fields produced by these two coils are given by

$$\begin{aligned} B_{gz} &= (0, -Gy, Gz) \\ B_{gy} &= (0, Gz, Gy) \end{aligned} \tag{1}$$

with gradient per unit current  $G/I = 2 \times 10^{-4}$  T/A m. The inductance of the coils is 84  $\mu$ H and the resistance is 0.4  $\Omega$ .

The  $x$  gradient is produced by a quadrupolar coil with the distribution of wires determined by a target field method.<sup>[24,25]</sup> The four loops, each with six windings, are on the surface of the 16 cm diameter cylinder coaxial with the detection coil. Such arrangement enables easy access to the probe area. In the first approximation, the field produced by this coil is

$$B_{gx} = (Gz, 0, -Gx) \quad (2)$$

with gradient per unit current  $G/I = 4.25 \times 10^{-4}$  T/A m. The inductance of the coil is 23.2  $\mu$ H and the resistance is 0.31  $\Omega$ . The length of the linear gradient region is 11 cm.

The NMR signal in a strong magnetic field is usually detected with low-inductance coils (small number of windings) because coils must be tuned to high Larmor frequency. The coils with a small number of windings produce low thermal noise, which increases with the fourth root of Larmor frequency (due to the skin effect). Sample induced thermal noise (caused by dissipation of induced currents) increases linearly with Larmor frequency. In a strong magnetic field, the sample induced thermal noise dominates coil's thermal noise. In our case, detecting coils with a high number of windings can be successfully used because the signal frequency is low. In Earth's magnetic field, sample induced noise can be neglected and even the coil thermal noise is often smaller than the noise induced by background electromagnetic field, unless the experiment is performed in an AF shielded environment. To some extent, rapid interferences of magnetic field usually caused by urban activities (railroad, electrical network, distant storms), can be reduced using gradiometric coils or shield coils. A grounded polarizing coil is employed as a shield.<sup>[26]</sup> The detecting coil is a solenoid (11 cm length, 11 cm diameter, 6000 windings) placed coaxially with the polarizing coil and perpendicular to Earth's magnetic field. The size of the detecting coil is limited by the  $x$  gradient coil. The large number of windings enhances the signal and the windings are wound in six sectors to minimize self-capacitance of the coil. The coil is connected to the pre-amplifier only during the signal acquisition. This is necessary because the coil amplifying electronics is sensitive to the current changes in all other coils (especially large polarizing current changes can damage the amplifier). The  $Q$  of the coil is deliberately lowered by a resistor to enable the detection of a signal from a 200 Hz bandwidth. A wider bandwidth receiving coil does not require sharp tuning to the signal frequency.

The signal from the detection coil is sampled either directly, or after quadrature detection with a 15 bit A/D converter, and sent to a PC for storage and further analysis. Besides the signal amplitude, both the phase and frequency of the signal are important and even necessary in imaging. The fluctuations in magnetic field affect the Larmor frequency, and these fluctuations hinder the detection of the phase and frequency of the signal. Random phase changes of the signal also attenuate the averaged signal. The phase and the frequency of the signal are controlled with AF pulses and magnetic field gradients, but in order to predict (calculate) the phase at a given time, the exact time variation of the Larmor frequency should be known. In a quadrature detection, common practice is to use AF (or radio-frequency in strong field) signal

generated by a stabilized oscillator, and to stabilize the static field by shim coils controlled by a signal from a proper probe (spin-lock signal) whenever phase stability is an issue. This method is inadequate in our case; the problem is Earth's magnetic field temporal instability. The field fluctuates by  $2.5 \times 10^{-8}$  T/year,  $5 \times 10^{-8}$  T/day, and  $10^{-9}$  T with a period of about 25 sec. These changes are caused by electric currents in Earth's core, fluctuations in ionosphere, sun activity, etc.<sup>[27,28]</sup> Since scanning is inherently slow because of the polarization period, changes in magnetic field are inevitable. Accurate detection of the signal phase, using a fixed-frequency reference oscillator, is impossible and active shimming of slow field fluctuations is practically challenging. This problem is circumvented by using a reference oscillating signal provided by a separate NMR spectrometer. The construction of the reference spectrometer is simple, since providing the free induction signal is the only requirement imposed. The spectrometer, placed some 20m from the imaging coils, experiences similar  $B_0$  but does not disturb the measurement. It consists of two solenoids placed next to one another; their symmetry axes are perpendicular to  $B_0$  (parallel to the symmetry axis of the detecting coil). Each coil contains water-filled 1 L bottles. The coils are connected in a series but oriented in gradiometric arrangement to improve  $S/N$ . The reference coils perform two tasks: they are used for polarization of the sample and to detect free induction decay. The 1 A polarizing current can be turned on and off by a transistor switch. The coils are tuned to the Larmor frequency with high  $Q$ -value. The magnetization is induced in the direction perpendicular to  $B_0$  (along the symmetry axes of the coils). The variable resistor connected to the polarizing-current source in a series with coils slightly below critical damps the polarizing current until the switch turns off. As the current in the coils decays after a few oscillations, the magnetization remains in the plane perpendicular to  $B_0$  and free induction signal is induced. In such case, excitation AF pulses are not required. The polarizing field of the reference coils is switched off before the polarizing field of the imaging coils, since the reference signal is needed for the AF excitation pulse. The reference signal used for the quadrature detection<sup>[8-10]</sup> is given by

$$s_r = s_{0r} \sin(\omega_0 t + \omega_f t + \varphi_f + \varphi_r)$$

Here,  $\omega_0$  is the average Larmor frequency,  $\omega_f$  represents the fluctuations in magnetic field,  $\varphi_f$  is a random phase induced by magnetic bursts, and  $\varphi_r$  is the phase of the undisturbed reference signal and can be set to 0. The signal shifted in phase by  $\pi/2$ , required for quadrature detection, is generated with a phase shifter.

To demonstrate the use of the reference signal in quadrature detection, one can write the signal  $s_m$  from a small part of the sample (voxel) as

$$s_m = s_{0m} \sin(\omega_0 t + \omega_f t + \omega_m t + \varphi_f + \varphi_m)$$

Here,  $\omega_m t$  is the phase generated by the magnetic field gradient applied during the signal acquisition (readout gradient) and  $\varphi_m$  is the phase of the signal generated by the gradient applied during the magnetization manipulation (phase gradient). We assume

that the field fluctuations at the location of the sample and reference coils are the same. After the quadrature detection of this signal, the real and imaginary parts  $s_r$  and  $s_i$  of the signal are, respectively,

$$s_r = \frac{1}{2} s_{0m} s_{0r} \cos(\omega_m t + \varphi_m - \varphi_r)$$

$$s_i = \frac{1}{2} s_{0m} s_{0r} \sin(\omega_m t + \varphi_m - \varphi_r)$$

The unwanted phase and frequency fluctuations cancel out. The signal of the complete magnetization is the sum (integral over the sample volume) of all partial magnetizations. The frequency and phase distribution of spins can be determined using inverse 2D Fourier transform<sup>[29]</sup> of  $\int (s_r + is_i) dV$ .

The experiments are controlled by a personal computer using a homemade pulse controller. The beat of the controller is 20 MHz, enabling a 0.5  $\mu$ sec time resolution, which is sufficient for our purpose. The controller uses four D/A converters for gradient and AF amplitude modulation, two A/D converters for the imaging and reference signal sampling, and four digital gates for controlling the polarization, reference, AF, and detection. In addition, the controller buffers sample data and communicates with a PC through a standard RS232 port.

To reduce electromagnetic interferences, the NMR system is located outside an urban area. Power supply and other electronics are located some 20 m from the system of coils and connected to the coils with coaxial cables. The coils are mounted in a wooden shack based on aluminum frame; no ferromagnetic material is used for construction since it can distort Earth's magnetic field.

## OVERVIEW

The NMR studies performed with the above-described system include: diffusion measurements,<sup>[30]</sup> imaging,<sup>[31]</sup> flow measurements combined with imaging of flow distribution,<sup>[32]</sup>  $T_1$  and  $T_2$  measurements, and contrast enhancement in imaging,<sup>[33]</sup> imaging of diffusion distribution,<sup>[34]</sup> natural convection,<sup>[35]</sup> and other more specialized unpublished experiments such as slice selection specific measurements.<sup>[36]</sup>

For the imaging experiments spin-warp imaging technique<sup>[37]</sup> is employed; some images are shown in Fig. 4. They show slices of different fruits: (a) apple, (b) orange, and (c) pepper. A typical scan takes on the order of an hour. With gradient coils, the field of view is limited to a maximum of 30 cm, the best resolution achieved so far is 2 mm/pixel. Flow measurements have been performed using different techniques such as spin warp, time of flight, wash in/out described elsewhere.<sup>[38–40]</sup> Examples of the flow measurements in Earth's magnetic field are shown in Fig. 5. Figure 6 shows a slice profile of water flowing in a cylindrical tube. From the slice profile and encoding parameters, the velocity can be determined. The relaxation times for different substances were also measured. The shortest measurable relaxation times are limited by the duration of excitation pulse to some 10 msec. The results are important since they differ from those in the strong field, since the relaxation is caused by field fluctuations at different frequency

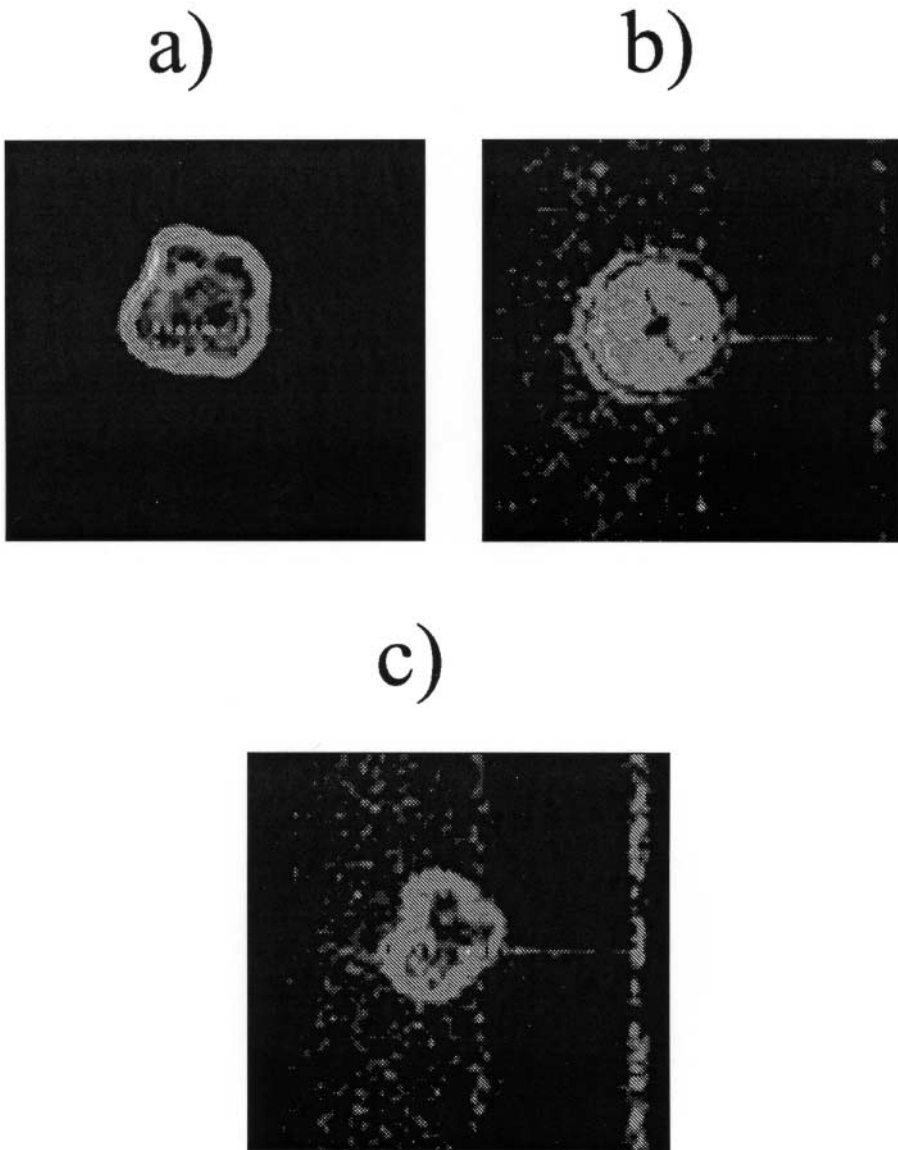


**Figure 4.** Images obtained with spin-warp imaging sequence in Earth's magnetic field: (a) apple, (b) orange, (c) pepper. The field of view is 15 cm with a resolution of  $64 \times 64$  pixel.

scales. Likewise, contrast in images can be improved as shown in Figs. 5–7.<sup>[33]</sup> The sequence used for these images employs spin-warp imaging technique combined with contrast enhancing techniques.<sup>[8–10]</sup> The diffusion measurements are quite simple yet specific, since  $B_0$  is on the same order of magnitude as gradient field. In Earth's magnetic field, the concomitant components of magnetic field cannot be neglected in certain cases.<sup>[30,41–43]</sup> Self-diffusion of different liquids was measured with PGSE<sup>[3,4,11–14]</sup>

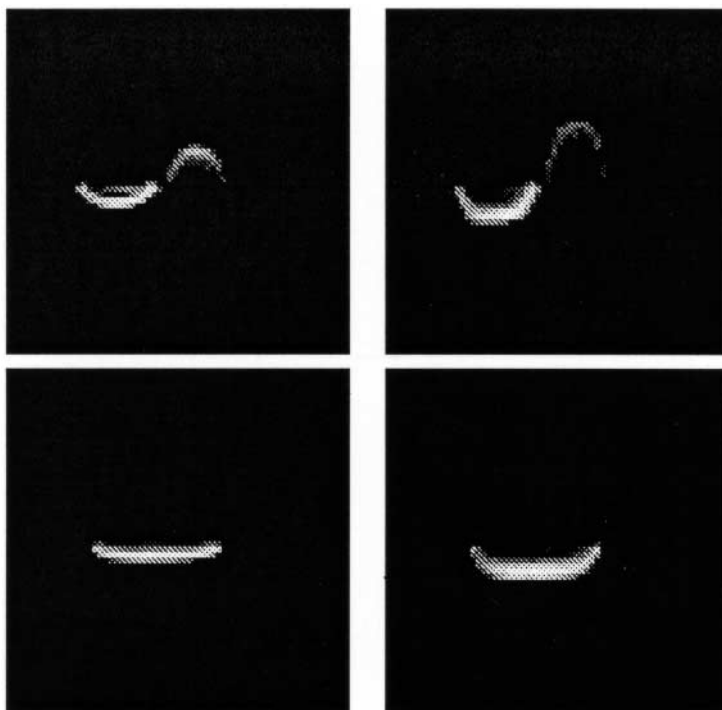


**Figure 5.** An example of flow measurements. The images show deformation in a plane slice of excited water spins after encoding time for counter-flows in two pipes (top) and a flow in a single pipe (bottom).

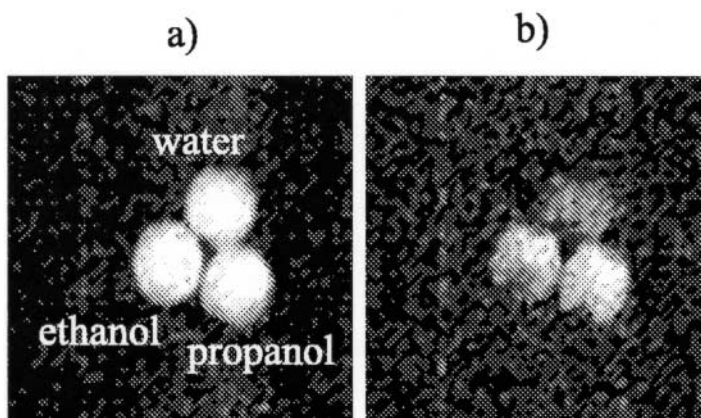


**Figure 6.** A  $64 \times 64$  pixel 2D image with 20 cm field of view showing the distribution of self-diffusion constant as measured with PGSE and spin warp combination: (a) no gradient, (b) with gradient (parts with higher self-diffusion constant become darker). The sample studied consists of three cylindrical tubes each 5 cm in diameter filled with water, ethanol, and propanol. A coronal slice through the sample is shown.

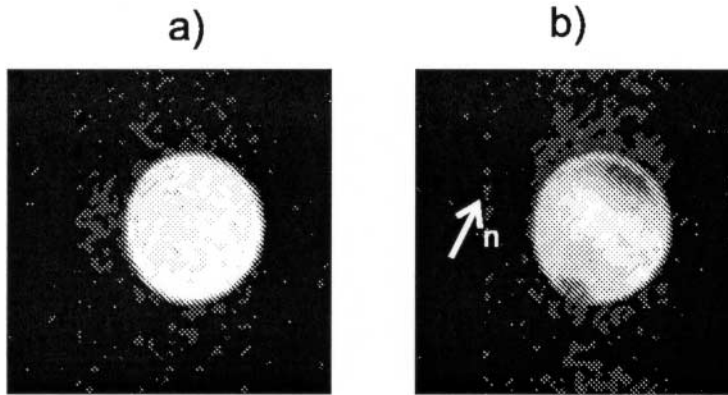


**Figure 7.** The coronal slice of a 10 cm diameter cylinder filled with propanol. Dark patches seen on the image that was scanned with gradient field turned on (a) image made without gradient. (b) The manifestation of natural convection. The arrow  $n$  indicates vertical.

methods. The range of diffusion constants is limited by a finite gradient strength of 0.02 T/m (and relaxation, which limits the encoding time). The distribution of diffusion constant was measured with a spin-warp imaging, preceded by PGSE sequence to enhance the diffusional contrast,<sup>[34]</sup> as shown in Fig. 6. The effect of natural convection was observed (Fig. 7) and investigated.<sup>[35]</sup>

## CONCLUSION

Measurements in Earth's magnetic field offer an inexpensive alternative to a strong field NMR. Weak  $B_0$  provides unique experimental conditions comparable only with NMR in a stray field of a superconducting magnet, where the effects of strong concomitant gradient components can be studied. In NMR, the "magnetic field gradient" is named a non-uniform magnetic field only when it is weaker than the main magnetic field,  $B_{z0}$ . According to Maxwell's equations, the direction of a non-uniform magnetic field is always changing. This means that there is always more than one component of the field different from zero. Therefore, the magnetic field at a point shifted from the initial position for  $dr$  can be written as

$$B = B_0 + B_g(r, t) = B_0 + G(t)dr$$

with  $G$  being a tensor. In the case of  $B_g(r, t) \gg B_{z0}$ , the magnetic field components perpendicular to the static magnetic field are neglected; index  $j$  stands for the individual spin. The magnetic field gradients are the remaining components of the tensor. This approximation has no meaning whenever the applied non-uniform magnetic field is of the order of, or larger than, the main magnetic field. However, in a weak main magnetic field the spin echo response

$$E(t) \approx \sum_j e^{i \int_0^t \omega_{\text{eff}}(r_j, t') dt'}$$

is governed by the effective precession frequency

$$\omega_{\text{eff}}(r_j, t) = \sqrt{(\omega_0 + \gamma B_{gz}(r_j, t))^2 + \gamma^2 B_{gx}^2(r_j, t) + \gamma^2 B_{gy}^2(r_j, t)}$$

whenever the magnetic field time-variation fulfills the adiabatic condition

$$\frac{d\omega_{\text{eff}}}{dt} \ll \omega_{\text{eff}}^2$$

Thus, in the first approximation, the signal in the vicinity of spin echo peak encodes spin location at  $r_j = r_{j0} + \Delta r_j$  as

$$E(t) \approx \sum_j e^{i \int_0^t \Delta r_j \nabla |\omega_{\text{eff}}(r_j, t')| dt'}$$

because  $\int_0^{2\tau} \omega_{\text{eff}}(r_{j0}, t) dt \approx 0$ ; the effective precession frequency changes sign upon application of a  $\pi$  RF pulse.

The magnetic field gradient caused by susceptibility mismatch is much smaller in a weak field, which results in a longer signal and helps to increase  $S/N$ . Also longitudinal and transversal relaxation is different, and measurements of relaxation give information on molecular dynamics outside the reach of strong field NMR. Furthermore, field uniformity enables use of large samples and with proper polarization, shielding and reference detection,  $S/N$  can be maintained at reasonably high values.

## REFERENCES

1. Bloch, F.; Hansen, W.W.; Packard, M. *Phys. Rev.* **1946**, *69*, 127.
2. Purcell, E.M.; Torrey, H.C.; Pound, R.V. *Phys. Rev.* **1946**, *69*, 37.
3. Hahn, E.L. *Phys. Rev.* **1950**, *80*, 580.
4. Carr, H.Y.; Purcell, E.M. *Phys. Rev.* **1954**, *94*, 630.
5. Lauterbur, P.C. *Nature* **1973**, *242*, 190.
6. Mansfield, P.; Granell, P.K. *J. Phys. C* **1973**, *69*, L422.
7. Kumar, A.; Welte, D.; Ernst, R.R. *J. Magn. Reson.* **1975**, *18*, 69.
8. Slichter, C.P. *Principles of Magnetic Resonance*; Springer-Verlag: Berlin, 1990.
9. Solomon, I. *Phys. Rev.* **1958**, *110*, 61.
10. Callaghan, P.T. *Principles of Nuclear Magnetic Resonance Microscopy*; Oxford University Press: Oxford, 1991.
11. Blombergen, N.; Purcell, E.M.; Pound, R.V. *Phys. Rev.* **1948**, *73*, 679.
12. Torrey, H.C. *Phys. Rev.* **1956**, *104*, 563.
13. Stejskal, E.O. *J. Chem. Phys.* **1965**, *43*, 3597.
14. Stejskal, E.O.; Tanner, J.E. *J. Chem. Phys.* **1965**, *42*, 288.
15. Stilbs, P. *Progr. Nucl. Magn. Reson. Spectrosc.* **1987**, *19*, 1.
16. Packard, M.E.; Varian, R. *Phys. Rev. A* **1954**, *94*, 941.
17. Melton, B.F.; Pollak, V.L. *Rev. Sci. Instrum.* **1971**, *42*, 769.
18. Callaghan, P.T.; Le Gros, M. *Am. J. Phys.* **1982**, *50*, 709.
19. Favre, B.; Bonche, J.P.; Mehier, H.; Peyrin, J.O. *Magn. Reson. Med.* **1990**, *13*, 299.
20. Kleinberg, R.L. *Encyclopedia of Magnetic Resonance*; Wiley: New York, 1995.

21. Melton, B.F.; Pollak, V.L.; Mayes, T.W.; Willis, B.L. *J. Magn. Reson. A* **1996**, *117*, 164.
22. Trushkin, D.V.; Shushakov, O.A.; Legchenko, A.V. *Geophys. Prospect.* **1994**, *42*, 855.
23. Callaghan, P.T.; Eccles, C.D.; Seymour, J.D. *Rev. Sci. Instrum.* **1997**, *68*, 4263.
24. Oedberg, G.; Oedberg, L. *J. Magn. Reson.* **1974**, *16*, 342.
25. Planinšič, G. University of Ljubljana, 1993; Ph. D. Thesis.
26. Planinšič, G. *J. Magn. Reson.* **1997**, *126*, 30.
27. Bene, G.J. *Phys. Rep.* **1980**, *58*, 213.
28. Chapman, S. *The Earth's Magnetism*; Methuen: London, 1951.
29. Press, W.H.; Flannery, B.P.; Teukolsky, S.A.; Vetterling, W.T. *Numerical Recipes*; Cambridge University Press: Cambridge, 1990.
30. Stepišnik, J.; Kos, M.; Planinšič, G.; Eržen, V. *J. Magn. Reson. A* **1994**, *107*, 167.
31. Stepišnik, J.; Eržen, V.; Kos, M. *Magn. Reson. Med.* **1990**, *15*, 386.
32. Kos, M. University of Ljubljana, 1992; Ph. D. Thesis.
33. Planinšič, G.; Stepišnik, J.; Kos, M. *J. Magn. Reson. A* **1994**, *110*, 170.
34. Mohorič, A.; Stepišnik, J.; Kos, M.; Planinšič, G. *J. Magn. Reson.* **1999**, *136*, 22.
35. Mohorič, A.; Stepišnik, J. *Phys. Rev. E* **2000**, *62*, 6615.
36. Duh, A. University of Ljubljana, ; 1994; B. Sc. Thesis.
37. Edelstein, E.A.; Hutchinson, J.M.S.; Johnson, G.; Redpath, T. *Phys. Med. Biol.* **1980**, *25*, 751.
38. Nalcioglu, O. *Phys. Med.* **1990**, *6*, 175.
39. Caprihan, A.; Fukushima, E. *Phys. Rep.* **1990**, *198*, 195.
40. James, T.L.; Margulis, A.R. Eds.; *Biomedical Magnetic Resonance*; Radiology Research and Education Foundation: San Francisco, 1984.
41. Stepišnik, J. *Progr. NMR Spectrosc.* **1985**, *17*, 187–209.
42. Stepišnik, J. *Phys. B* **1994**, *198*, 299.
43. Stepišnik, J.Z. *Phys. Chem.* **1995**, *190*, 51.

Received August 1, 2003

Accepted February 25, 2004

Manuscript 1399

Copyright of Instrumentation Science & Technology is the property of Marcel Dekker Inc. and its content may not be copied or emailed to multiple sites or posted to a listserv without the copyright holder's express written permission. However, users may print, download, or email articles for individual use.